Pramāṇa – J. Phys., Vol. 25, No. 1, July 1985, pp. 29–41. © Printed in India.

Track recording properties of soda glass detector for accelerated heavy ions

S M FARID

Department of Physics, Rajshahi University, Rajshahi, Bangladesh

MS received 3 October 1984; revised 9 April 1985

Abstract. The etch pit diameters of soda glass detector samples exposed to $^{132}_{54}$Xe-ions of different energies are measured for different etching times after etching the detector in a 'new etchant' free of the adverse effect of the etch product layer. The dependence of track diameter on the energy and on the energy loss, dE/dx of $^{132}_{54}$Xe-ion in soda glass has been presented. The energy resolution of soda glass and the critical angle for etching of fission fragment tracks in glass detectors have also been determined. The maximum etched track length of $^{132}_{54}$Xe-ion in soda glass has been compared with the theoretical range. The effects of different annealing conditions on bulk etch rate of glass detector and on diameters of $^{132}_{54}$Xe-ion tracks have been presented. Experimental results show that there is a decrease in track etch rate, etching efficiency and etchable range of $^{132}_{54}$Xe-ions with annealing. The annealing of oblique tracks shows that the vertical tracks are more stable than the oblique tracks.

Keywords. Glass detector; energy resolution; critical angle; response curve; etching efficiency; diameter distribution; annealing.

PACS No. 29·40

1. Introduction

Solid state nuclear track detectors (SSNTDs) have been extensively studied in the recent years both with regard to their practical applications in diverse fields such as nuclear physics, earth and space physics, biology, dosimetry and many others and as a tool for studies of basic phenomena (Fleischer *et al* 1975). The glass detectors have a special place among the SSNTDs due to their better homogeneity, transparency and relatively high threshold for registration of nuclear charged particles. Charged particles generally produce tracks in glasses with high contrast and sharp and circular etch pit edges. Therefore, it is possible not only to detect particles but also to obtain further information about the kinetic energy and the nuclear charge of the heavy ions by measuring the lengths of the tracks and the diameters respectively (Fleischer *et al* 1975; Fiedler *et al* 1980). SSNTDs subjected to high temperatures after irradiation, but before etching, produces an apparent reduction of particle track length as well as its diameter (Khan and Durrani 1972). Hence, for accurate track analysis, proper temperature-dependent correction to the efficiency factor must be applied.

In the present paper we present the results of our study using a 'new etchant' (Farid and Sharma 1982). The track diameter variation with etching time and particle energy, energy resolution and critical angle for registration have been studied. The energy loss, dE/dx has been calculated in soda glass detector and has been correlated with track

diameter. This paper also describes the results of the annealing experiments carried out on the $^{132}_{54}$ Xe-ion tracks in soda glass detector.

2. Experimental procedure

Soda lime glass samples exposed to $^{132}_{54}$ Xe-ions (table 1) have been obtained from JINR, Dubna (USSR). The energy of $^{132}_{54}$ Xe-ions is varied by inserting Al-foils of different thicknesses in the path of the ions. The angles of exposure are 90° and 45° with respect to the detector surface. The annealed and unannealed samples are etched in the 'new etchant' (Farid and Sharma 1982) [HF (12 by vol %) + H_2SO_4 (24 %) + H_2O in the ratio 12:2:9] in a plastic vessel which is kept in a constant temperature water bath. The track diameter is measured with a transmitted light microscope having an eyepiece micrometer of least count (LC) = 0·215 μm at a magnification of 900 ×. The absence of error bars in all the figures represents the accuracy better than the size of the symbols used in the figures.

3. Results and discussions

3.1 *Variation of diameter with etching time*

In figure 1, the mean track diameters of vertical tracks are plotted as a function of etching times with the particle energy as parameter for an etching temperature of 30°C. The beginning of the curve where the slope changes continuously is due to the track etch rate (V_t) as well as due to shape of the tracks and in the second part of the curve the track diameter (the tracks remaining spherical in this phase) increases (Somogyi and Szalay 1973) according to the relation $D \propto t^{1/2}$, where t is the etching time. The plot (not shown) of mean track diameter of $^{132}_{54}$ Xe-ion tracks with etching time at different temperature shows that for a given etching time the diameter increases rapidly with etching temperature. This is obviously due to increased etch rates at higher temperatures. The plot of mean track diameter as a function of energy with etching time as parameter is shown in figure 2. These values are taken from the curves in figure 1. With large etching times, the diameters continue to increase with increasing energy. This is on account of the fact that the rate of energy loss, dE/dx of the ion increases (up to the peak value in the dE/dx vs E curve) with increasing energy of the ion and hence

Table 1. Exposure conditions of $^{132}_{54}$ Xe-ions.

Detector	Energy (MeV)	Angle of exposure (w.r.t detector surface)
Soda lime glass	126·7	90°
	85·7	90°
	65·0	90°
	52·0	90°
	85·7	45°

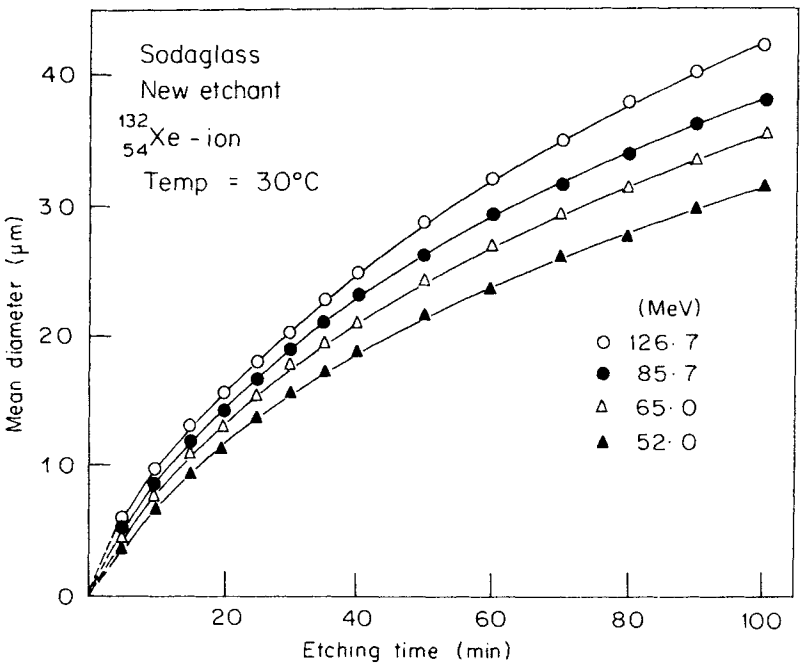

Figure 1. Variation of track diameter with etching time for $^{132}_{54}$Xe-ions of different energy in soda glass detector etched in the 'new etchant' at 30°C.

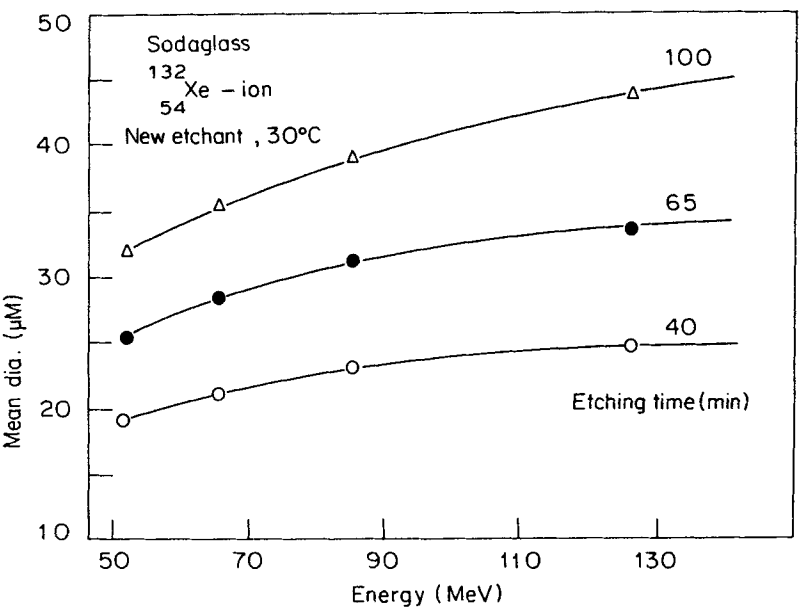

Figure 2. Variation of track diameter with energy of $^{132}_{54}$Xe-ions in soda glass detector etched in the 'new etchant' at 30°C for different etching times.

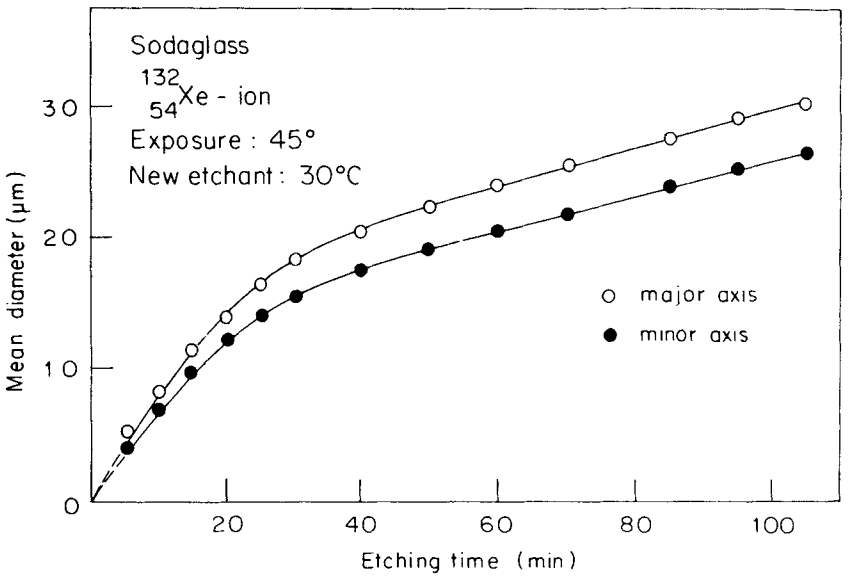

Figure 3. Variation of mean major and mean minor axes diameter with etching time for $^{132}_{54}$Xe-ion tracks in soda glass detector.

the track etch rate, V_t increases and consequently the track diameter increases. The slope of the diameter *vs* energy curve increases with etching time. This indicates that the ion of the same charge and mass but with different energies can be resolved easily if the etching time is large. This also shows that the energy resolution of the glass detector is improved when diameters are etched as large as possible. It is observed from figure 2 that the samples etched for 100 min show a maximum slope, thereby indicating a better resolution. Figure 3 shows the variation of mean major and mean minor axes of etchpit diameters of 85·7 MeV $^{132}_{54}$Xe-ion tracks *vs* etching time in case of tracks inclined at 45° angle of incidence, when the etching is carried out in the 'new etchant' at 30°C.

3.2 *Energy resolution of glass detector*

The energy-loss, dE/dx of $^{132}_{54}$Xe-ions in soda glass is computed by using the range and stopping power equations of Mukherji and Nayak (1979). In figure 4 $\ln D$ has been plotted as a function of dE/dx for $^{132}_{54}$Xe-ion tracks in soda glass etched in the 'new etchant' for different temperatures. This shows the exponential variation of D with dE/dx. The diameters for different temperatures have been taken for a 110·5 μm surface removal of each detector surface. Similar plots (not shown) have also been drawn for different surface removals of each detector surface. It is concluded that the diameter depends only on the energy-loss and not on the etching temperature. If we take into account all our experimental limitations and calculate the minimum diameter difference which is distinguishable under our experimental set up, we can find the possible energy resolution corresponding to the curve in figure 4 (Sharma *et al* 1981) for the soda glass detector for given etching conditions. For our experimental set up, the minimum distinguishable diameter difference appears to be $\sim$ 1·50 μm. From figure 4 we have calculated the resolution limit corresponding to this value of diameter

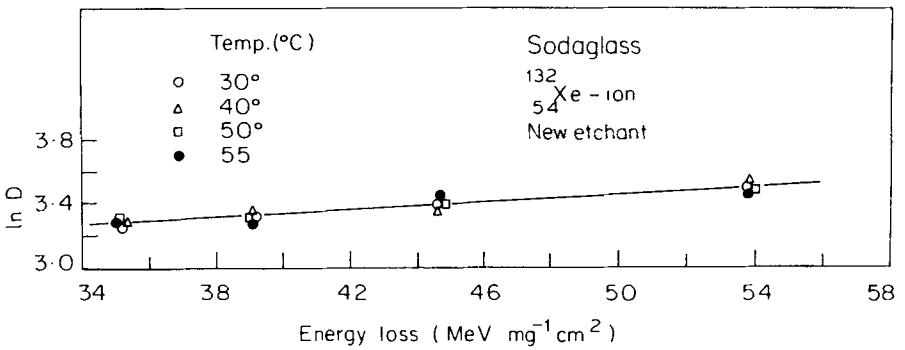

Figure 4. Variation of ln D with energy loss, dE/dx of $^{132}_{54}$Xe-ions in soda glass detector for different temperatures of the 'new etchant'.

Table 2. Energy resolution and critical angle of etching for soda glass detectors using different etchants.

Etchant and etching temperature	Ion	Energy resolution (MeV)	Critical angle of etching (degree)
HF (40 vol%), 40°C	$^{132}_{54}$ Xe	8[a]	40[a]
HF (48 vol%) + H_2SO_4 (96%) + H_2O in the ratio 6:1:18 with Zinc, 40°C	Fission fragment from $^{252}_{98}$ Cf	—	37[b]
New etchant [HF (12 vol%) + H_2SO_4 (24%) + H_2O in the ratio 12:2:9], 30°C	$^{132}_{54}$ Xe	4[c]	
New etchant	Fission fragement from $^{252}_{98}$ Cf		28[c]

[a]Sharma *et al* (1981); [b]Singh (1981); [c]Present study.

difference for $^{132}_{54}$ Xe-ion tracks in soda glass detector using our new etchant. Following the procedure of Khan and Durrani (1972, 1973) we have determined the critical angle for etching of fission fragment tracks in soda glass. The results are presented in table 2. The energy resolution and critical angle of etching for soda glass obtained by other workers (Sharma *et al* 1981; Singh 1981) are also shown in the same table for comparison. We observe that the use of the new etchant improves the energy resolution of soda glass by a factor 2.

3.3 *Response of soda glass detector*

A sample irradiated vertically to $^{132}_{54}$ Xe-ions is etched in the 'new etchant' at 30°C for a short time, t_1. The track lengths are measured by a Z-motion of the microscope (Dwivedi 1979; Gomber 1980; Price and Fleischer 1971). Now another sample exposed vertically to $^{132}_{54}$ Xe-ions is etched for another short time, t_2 ($t_2 > t_1$), and the track lengths are measured. The true track length, L for each etching time is calculated by (Dwivedi 1979; Gomber 1980; Price and Fleischer 1971).

$$L = l + V_b t - V_b (t - t_c), \tag{1}$$

where l = observed length, V_b = bulk etch rate, t = etching time and t_c = complete etching time.

The average value of track etch rate at different points of the track is obtained by (Dwivedi 1979; Farid and Sharma 1984; Gomber 1980)

$$V_t = L/t. \tag{2}$$

The energy-loss, dE/dx of $^{132}_{54}$ Xe-ions at different penetration depths is computed using range and stopping power equations of Mukherji and Nayak (1979). The variation of $V = V_t/V_b$ with dE/dx of $^{132}_{54}$ Xe-ion in the soda glass detector is shown in figure 5.

3.4 *Range of $^{132}_{54}$ Xe-ion in soda glass detector*

Following the procedure discussed above the maximum etched track lengths of $^{132}_{54}$ Xe-ions of different energies in soda glass are determined which are presented in table 3. The theoretical range of $^{132}_{54}$ Xe-ions in soda glass is computed (table 3) using the range equations of Mukherji and Nayak (1979). The range of $^{132}_{54}$ Xe-ion in soda glass can be determined from the plot of the square of the diameter, D vs surface removal of the

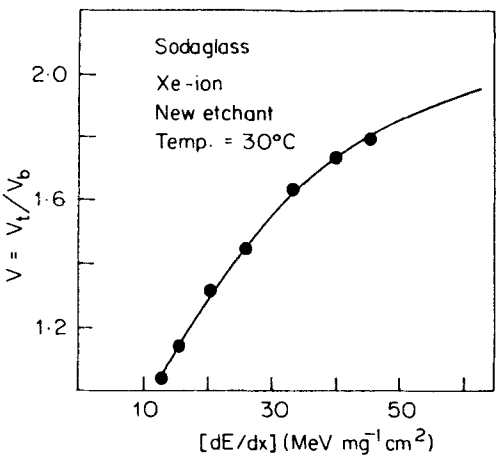

Figure 5. Dependence of $V = V_t/V_b$ on the energy loss, dE/dx of $^{132}_{54}$Xe-ion in soda glass detector etched in the 'new etchant' at 30°C.

Table 3. Range of $^{132}_{54}$Xe-ions in soda glass detector.

	Range (μm)		
Energy (MeV)	Theoretical (computed)	$D^2 - h$ method	Track length method
126·7	22·71	20·05 ± 1·25	19·95 ± 1·04
85·7	18·76	16·76 ± 1·10	16·91 ± 1·02
65·0	15·57	13·25 ± 1·04	13·42 ± 1·01

detector, h ($h = V_b t$). The D^2–h curves for $^{132}_{54}$Xe-ions in glass detector are drawn (not shown). Using this D^2–h method (Somogyi and Szalay 1973; Yayashi and Iwata 1981) the ranges of $^{132}_{54}$Xe-ions of different energies in soda glass are also calculated. These values are also given in table 3 for comparison. A good agreement is found between the ranges obtained by the track length method and the D^2–h method.

4. Annealing of $^{132}_{54}$Xe-ion tracks in soda glass

4.1 *Effect of annealing time and temperature on diameter of* $^{132}_{54}$*Xe-ion tracks*

Soda glass samples exposed vertically to 126·7 MeV $^{132}_{54}$Xe-ions are annealed for different time- temperature combinations. The annealed samples are then etched in the 'new etchant' at 30°C and the track diameters measured in each case. The effect of annealing time on track diameter is shown in figure 6 for a constant (260°C) annealing temperature. Similar experiments have also been done for annealing temperatures of 300, 190 and 150°C. The D–t plots for these annealing temperatures are not shown here because they display a similar trend in diameter reduction with annealing time.

The mean track diameter *vs* etching time curves for different annealing temperatures, keeping the annealing time constant (10 min), are shown in figure 7. Similar D–t curves are also drawn for different constant annealing times. These plots are not presented here. All these figures show a similar trend, *i.e.* the track diameter reduces with an

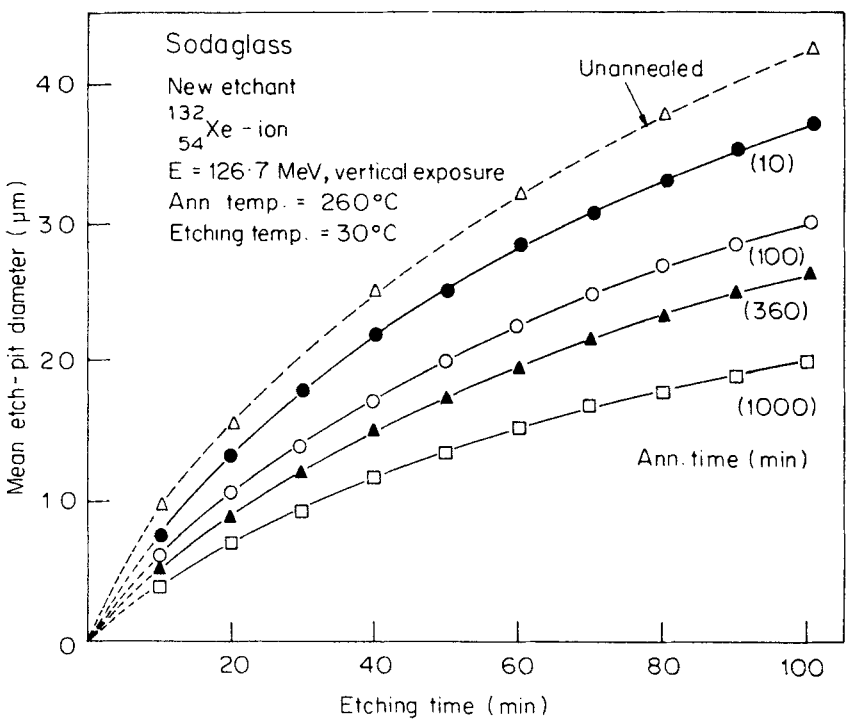

Figure 6. Variation of mean diameter of $^{132}_{54}$Xe-ion tracks with etching time for samples annealed at 260°C for different times.

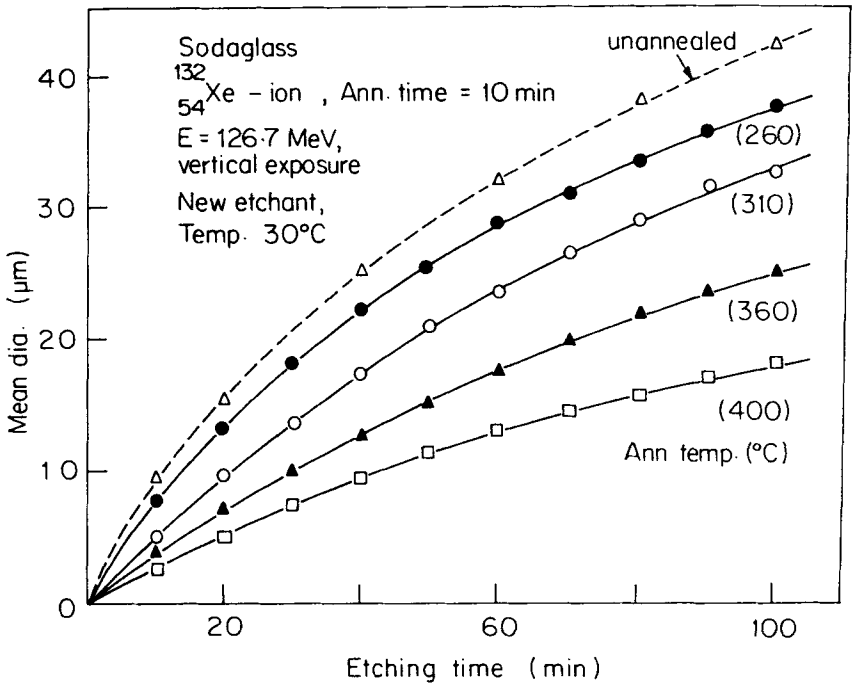

Figure 7. Variation of mean diameter of $^{132}_{54}$Xe-ion tracks with etching time for samples annealed for 10 min at different temperatures.

increase in the annealing temperature. Figure 8 shows the variation of track diameter corresponding to 50 min etching with annealing time t. A plot of diameter, D *vs* ln t is a straight line. The lines corresponding to smaller annealing temperatures lie above those corresponding to the higher annealing temperatures. The slopes of these lines have been found to increase with annealing temperature. On extrapolating, the different lines meet at a point which gives the diameter equal to the unannealed magnitude. The extrapolation gives the time for complete erasure of the tracks at different annealing temperatures. It is clear that for total fading of the tracks (*i.e.* $D = 0$), the annealing time at higher annealing temperatures will be less as compared to the time at lower temperatures.

4.2 *Effect of annealing on etch rates and etching efficiency*

Unexposed samples of glass detector are annealed at different temperatures for 1 hr. The samples are then etched simultaneously in the 'new etchant' at 30°C. The removed layers of the sheets are measured with a microthickness gauge having a LC ~ 0·5 μm. Experimental results show that there is no change in the bulk etch rate, V_b even at an annealing temperature of 350°C.

Now the detector samples which have been exposed to 126·7 MeV $^{132}_{54}$Xe-ions are annealed for different time-temperature combinations. The annealed samples are then etched simultaneously at 30°C for a particular time so that the removed layer from a single surface of the detector is $h = V_b t = 17$ μm. The mean diameter of 100 tracks has been determined in each case. The track etch rates are calculated from the relation

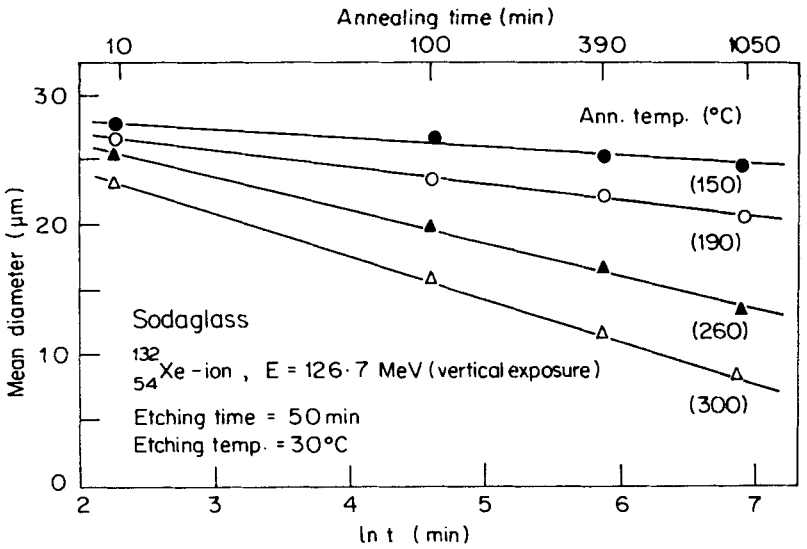

Figure 8. Plot of mean diameter of $^{132}_{54}$Xe-ion tracks corresponding to 50 min etching with annealing time t when annealed at different temperatures.

Table 4. Etch rate ratio and efficiency of $^{132}_{54}$Xe-ion tracks incident vertically on soda glass detector annealed at various temperatures.

Annealing temperatures (°C)	Annealing time (min)	Etch rate ratio (V)	Etching efficiency (η %)
Room temperature	0	1·73	42·20
153 ± 3	10	1·69	40·83
190 ± 3	10	1·63	38·66
260 ± 3	10	1·51	33·86
300 ± 3	10	1·43	30·26
300 ± 3	100	1·19	16·02

(Somogyi and Szalay 1973; Farid and Sharma 1982).

$$V_t = V_b[(4V_b^2t^2 + D^2)/(4V_b^2t^2 - D^2)]. \tag{3}$$

The etching efficiency, η is calculated (Khan and Durrani 1973) by

$$\eta = 1 - \frac{V_b}{V_t}. \tag{4}$$

These values are given in table 4. Both the track etch rate V_t and etching efficiency η have been found to decrease with annealing.

4.3 *Effect of annealing temperature on range of* $^{132}_{54}$*Xe-ion*

The detector samples exposed to 126·7 MeV $^{132}_{54}$Xe-ions are annealed for 1 hr at different temperatures. The annealed samples are etched in the 'new etchant' at 30°C for

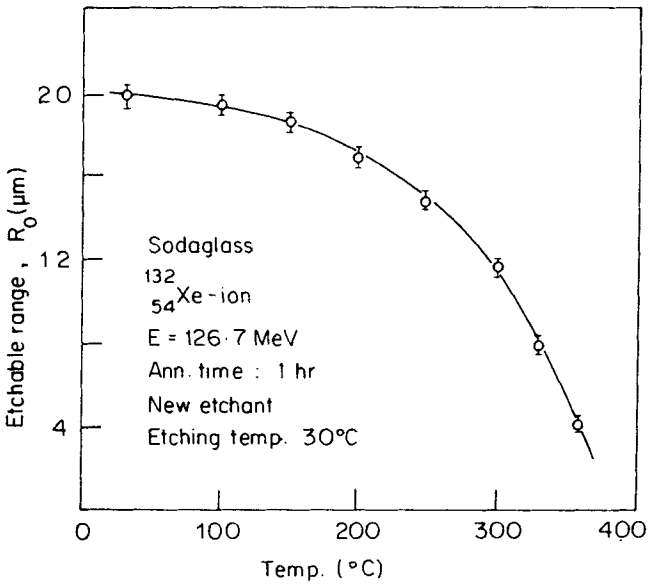

Figure 9. Variation of etchable range of $^{132}_{54}$Xe-ions in soda glass detector with annealing temperature.

different times. Each time the mean of 100 track diameters is noted. Using $D^2 - h$ method, the range is determined for different annealing temperatures. The results are shown in figure 9 where the mean range is plotted against annealing temperature. Clearly there is a decrease in the range with increase in annealing temperature.

4.4 *Effect of annealing temperature on diameter distribution*

Exposed glass samples are annealed at 275°C for 10 min. The annealed and unannealed samples are etched simultaneously for 30 min in the 'new etchant' at 30°C. The track diameter and track density are measured with an optical microscope. It is observed that with annealing not only the track density is reduced, but also the diameters of etched $^{132}_{54}$Xe-ion tracks are diminished as a result of lower etching velocity in the damage trail. Thus the latent damage caused by highly charged particle is effectively cured by heating the detector.

4.5 *Annealing of oblique tracks in soda glass detector*

Soda glass samples exposed to $^{132}_{54}$Xe-ions of energy 85·7 MeV at angles of 90° and 45° to the detector surface have been annealed for different time-temperature combinations. The annealed samples are etched simultaneously in the 'new etchant' at 30°C. Circular and elliptical tracks are observed respectively for 90° and 45° exposures. The etchpit diameters are measured in each case with the microscope.

Figure 10a shows the variation of mean major axis of elliptical etchpit diameters *vs* etching time for different annealing times for annealing temperature of 200°C. The effect of annealing time on etchpit diameter of vertical tracks for the same annealing temperature (200°C) is shown in figure 10b.

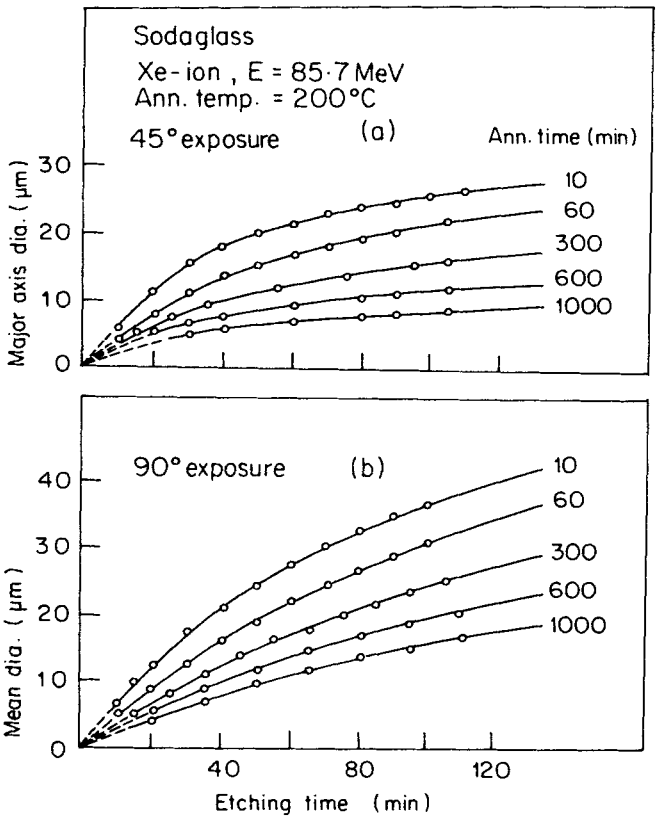

Figure 10. Variation of **a.** mean major axis diameter and **b.** mean diameter of $^{132}_{54}$Xe-ion tracks with etching time for different annealing times.

The effect of annealing temperature on etchpit diameters has been studied by plotting etchpit diameter of vertical tracks *vs* etching time curves at different annealing temperatures (figure 11a), at constant annealing time (10 min). The effect of annealing temperature on inclined tracks is shown in figure 11b. The annealing time is again 10 min in this case. These figures clearly show that the diameters of oblique tracks decrease at a faster rate with annealing time/annealing temperature as compared to the diameter decrease of vertical tracks. This means that the circular etchpits produced by perpendicular impacts will be more stable towards thermal treatments as compared to those of the elliptical etchpits produced by oblique impacts.

To verify the above conclusion, separate experiments are performed to study the variation of mean etchpit diameter in case of circular tracks and the mean major axis in case of elliptical tracks as a function of annealing temperature (keeping annealing time constant, 10 min) and as a function of annealing time (keeping annealing temperature constant, 200°C). The results are shown in figure 12. Figure 12a shows that the elliptical tracks are completely erased when annealed for 10 min at 375°C. The vertical tracks are more resistant and require a still higher temperature for their complete erasure. Figure 12b shows the effect of annealing at 200°C for different durations in case of tracks due to

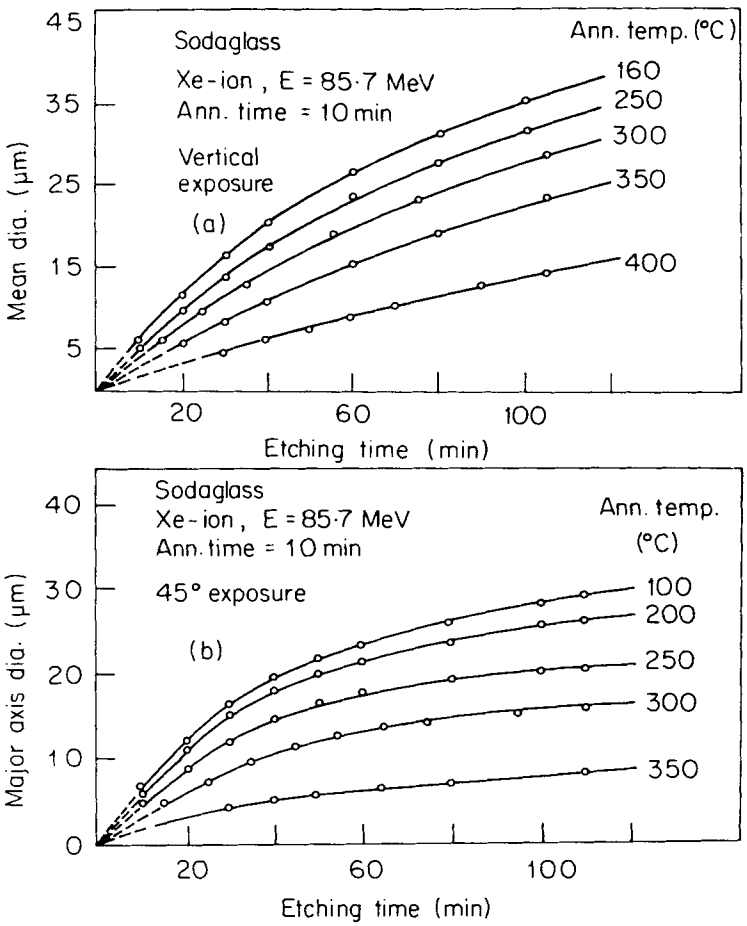

Figure 11. Variation of **a.** mean diameter and **b.** mean major axis diameter of $^{132}_{54}$Xe-ions with etching times for different annealing temperatures.

45° and 90° angle of incidence. This again confirms that the vertical tracks are stable for longer periods than the oblique tracks.

For track registration, $\phi > \phi_c$ where ϕ is the dip angle and ϕ_c is the critical angle of registration. As V_t is reduced by annealing, $V_t \sin \phi$ decreases and becomes less than V_b. The tracks are, therefore, not etched. If the angle of incidence is decreased from 90°, the condition $V_t \sin \phi > V_b$ will be violated first by tracks with smaller ϕ. As the annealing is further intensified, the tracks with large value of ϕ will also be erased and finally when ϕ_c approaches 90°, the vertically incident tracks are also erased.

Thus the subjection of a glass detector to high temperature after irradiation, but before etching, produces an alteration in the damaged region which results in latent track shrinkage (both radial and axial) and a reduction of etching velocity along the track (V_t). Therefore, a proper time-temperature dependent correction must be applied in experiments where the glass detectors are required to operate at a temperature higher than normal room temperature.

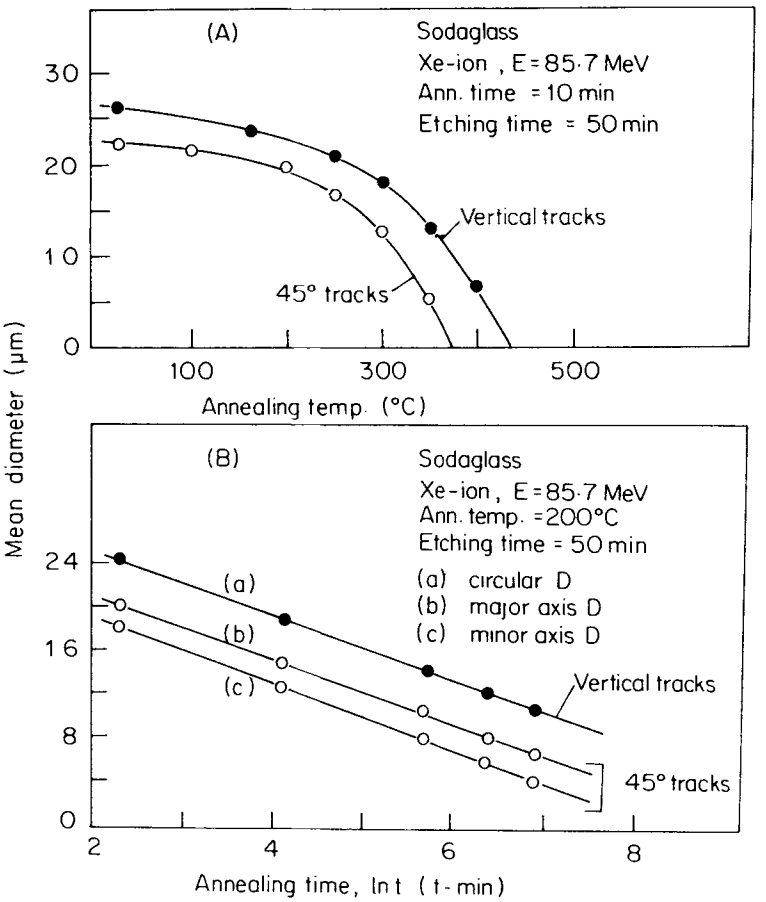

Figure 12. Variation of mean diameter of $^{132}_{54}$Xe-ion tracks with **a.** annealing temperature and **b.** annealing time for different angles of irradiation.

References

Dwivedi K K and Mukherji S 1979 *Nucl. Instrum. Method* **161** 317

Dwivedi K K 1979 *Study of heavy ion tracks in solid dielectric track detectors.* Ph.D. Thesis, IIT, Kanpur, India

Fleischer R L, Price P B and Walker R M 1975 *Nuclear tracks in solids* (Berkeley: University of California Press)

Fiedler G, Steinhauser V, Rautenberg T, Haag R and Gottschalk P A 1980 *Nucl. Instrum. Method* **173** 85

Farid S M and Sharma A P 1982 *Nucl. Tracks* **6** 175

Farid S M and Sharma A P 1984 *Radiat. Eff.* **80** 121

Gomber K L 1980 *Study of heavy ion tracks in glass detector* Ph.D. Thesis, Kurukshetra University, India

Khan H A and Durrani S A 1972 *Nucl. Instrum. Method* **98** 229

Khan H A and Durrani S A 1973 *Nucl. Instrum. Method* **113** 51

Mukherji S and Nayak A K 1979 *Nucl. Instrum. Method* **159** 421

Price P B and Fleischer R L 1971 *Annu. Rev. Nucl. Sci.* **21** 295

Somogyi G and Szalay S A 1973 *Nucl. Instrum. Method* **109** 211

Sharma A P, Yadav J S, Gomber K L, Perelygin V P and Stetsenko S G 1981 *Proc. 11th. Int. Conf. on SSNTDs* Bristol (UK) (Oxford: Pergamon Press) 321–324

Singh V P 1981 *Study of some environmental effects on heavy ion tracks in soda glass detector* Ph.D. Thesis, Kurukshetra University, India

Yayashi S and Iwata S 1981 *Radiat. Eff.* **54** 243